IMPROVEMENT OF THERMO-MECHANICAL PROPERTIES OF CERAMIC MATERIALS FOR NUCLEAR APPLICATIONS

Guy-Marc DECROIX, Dominique GOSSET, Bernard KRYGER
CEA-CEN Saclay,DMT/SETIC/LEMA, F-91191 Gif sur Yvette cedex, France
Michel BOUSSUGE, Hélène BURLET
Ecole des Mines de Paris, BP 87, F-91003 Evry cedex, France

In order to improve the thermo-mechanical properties of materials used as neutron absorbers in nuclear reactors, cermet or cercer have been produced with two original microstructures : micro- or macro-dispersed composites. The composites thermal shock resistance has been evaluated in an image furnace. The microstructures we obtained involve different reinforcement mechanisms, such as crack deflection, crack branching, crack bridging or microcrack toughening, and improvement of thermal conductivity. The results reveal a significant improvement of the thermo-mechanical properties of the boron base neutron absorbers whose fabrication process leads to a macro-dispersed microstructure.

1. INTRODUCTION

Neutron absorber materials are used for the power level control in nuclear reactors. The neutron absorption efficiency of ceramic boron compounds makes them the most common materials used in the control rods, mainly as boron carbide B_4C. The behavior of B_4C submitted to neutron irradiation is well known [1] : $^{10}B + {}^1n \rightarrow {}^4He + {}^7Li + 2.6$ MeV.

B_4C is most often used as high density cylindric pellets obtained by hot-pressing of fine grained powder, stacked in metallic sheath. However, this ceramic has poor thermo-mechanical properties and badly resists to accumulation of helium in the grain boundaries and to thermal stresses induced by the heat generation in a fast neutron flux (as in FBRs or advanced PWRs). The material swells and undergoes extended fracture[2,3]. Hence, its life time is not limited by the boron depletion but by the damage of the material itself.

In order to define the neutron absorbers for the new generation of nuclear reactors, new materials have been developped with improved thermo-mechanical properties ; the first requirement is a high neutron absorption efficiency, that means a high boron content. As it seems difficult to prevent cracking induced by helium generation, we aim to design a material in which cracks remain subcritical and propagate at short range, in order to prevent the complete damage of the pellets and maintain their integrity.

The toughening of brittle matrixes by the dispersion of a second phase provides composite materials with high properties only if the second phase material is appropriated. In this paper, original new composites are presented, ceramic-ceramic composites as B_4C-HfB_2 or B_4C-BN and ceramic-metal composites as B_4C-Mo or B_4C-Cu.

2. EXPERIMENTAL PROCEDURE

2.1. Materials elaboration

The materials are prepared by hot pressing from micronic powders (typical mean size in the range 5-10 μm). Thermo-mechanical properties of basic materials are reported in table I.

	B_4C	Mo	Cu	HfB_2	BN
^{10}B atoms/cm^3	8.9 10^{22}	-	-	5.5 10^{22}	
powder size	< 5 μm	5-8 μm	10 μm	5-10 μm	disc ϕ5 μm
Properties of dense hot pressed pellets (20°C)					
E (GPa)	400	320	110	500	70
σ_r (MPa)	370	600	-	400	310
ν	0.18	0.32	-	0.12	-
Thermal cond (W/m/K)	26	140	400	80	50
α (10^{-6}/°K)	4.5	5.2	16.5	6	6

TABLE 1
Properties of basic materials

The materials have been elaborated according to two different processes (figure 1)[4,5].

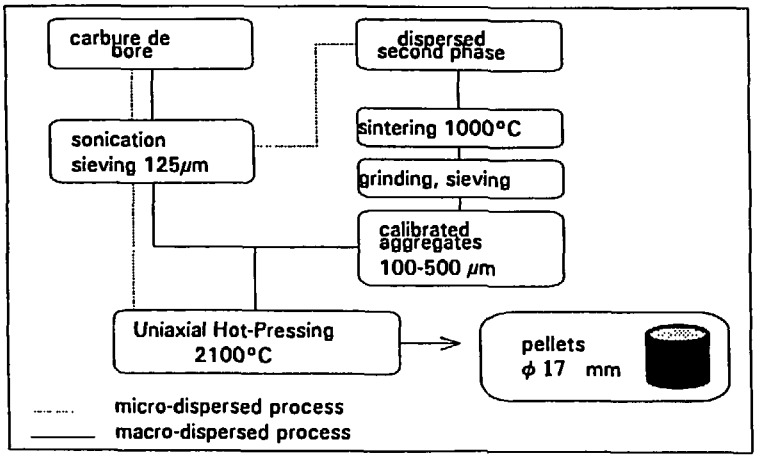

FIGURE. 1
Processing chart

The first one leads to a micro-dispersed microstructure, the second one to a macro-dispersed microstructure. In the first process, both components are dispersed by sonication (i.e. submitted to intense ultrasonic waves in a slurry), dried and sifted, in order to obtain a high homogeneity.

In the second process, the powder of the second phase is primarily sintered around 1000°C in vacuum, grinded and sieved to obtain nearly spherical aggregates of determined sizes, then mixed with sonicated B_4C powder.

Different aggregate sizes have been selected in the 100-500 μm range.

In order to keep a sufficient neutron absorption efficiency, the elaborated composites must have the highest boron content, compatible with a significant mechanical properties improvement. It is worth noting that Hf atoms are particularly interesting because of their high neutron absorption efficiency. Then, when the elaborated pellets can contain only from 10 to 30 volumic % of Mo, we can add from 10 to 50 volumic % of HfB_2 in the B_4C matrix.

Densification has been obtained by uniaxial hot-pressing at 2100 °C under vacuum in a graphite die. From the as-elaborated cylindrical pellets, thin discs (diameter 17 mm, thickness 1 mm) have been machined for structural, thermal and mechanical characterisations.

2.2. Thermal shock resistance

2.2.1 Test description

We have tested the thermal shock resistance of the different materials in an image furnace (figure 2). The disc sample is illuminated by two halogen spots and cooled at its periphery. Two ellipsoïdal reflectors focuse the light beam on the center of the sample.

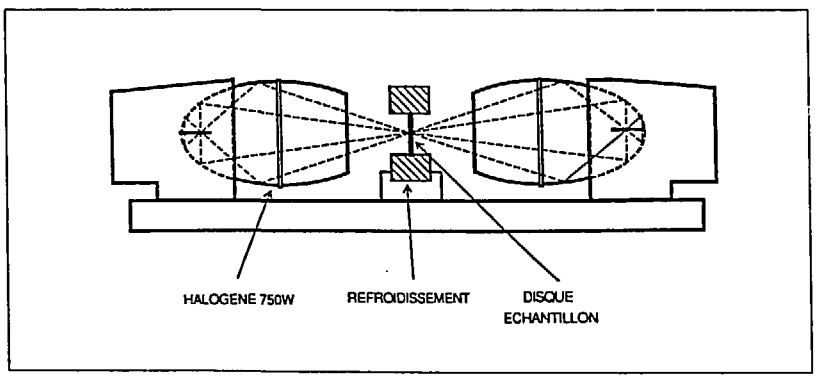

FIGURE 2
Schematic view of the image furnace

The lamps are connected in parallel and the applied voltage controlled. The heat power (W/mm^2) has been measured with a power meter. We have checked that heat power and voltage have been shown to be directly proportional.

Materials are submitted suddenly to increasing light powers, so far as they crack and/or break.

The temperature field on the disc surface is measured with a thermocouple translated from the periphery to the center ; the measured temperature has been checked by the observation of the melting of copper in a porous B_4C-20 vol.% Cu. This thermal shock device allows thermal drops between center and periphery to be obtained, which are in the same order of magnitude than those obtained in FBRs type reactor (up to 1000°C). The generated thermal stresses are then realistic.

2.2.2. Thermal profile calculation

The measured parabolic temperature profiles (figure 3) lead to the definitions of the critical temperature drop corresponding to the first damage of the sample, ΔT_d, and that corresponding to the sample fragmentation, ΔT_c, and allow the calculation of the maximal peripheric hoop stress.

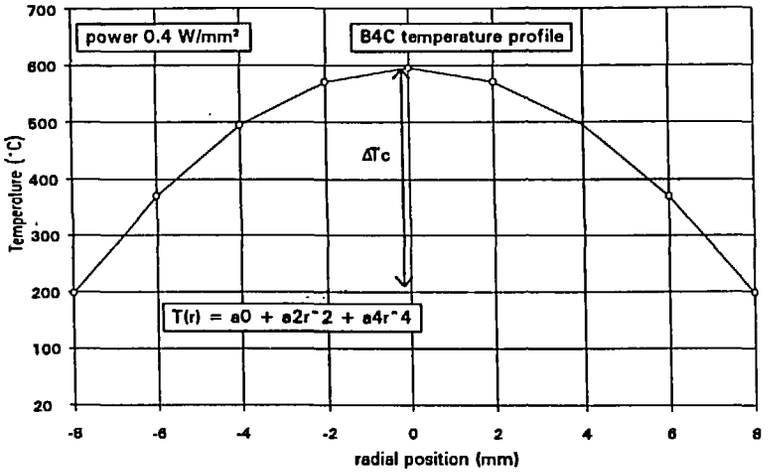

FIGURE 3
Temperature profile in a B_4C disc irradiated in the image furnace

Because the discs are very thin, temperature gradients in thickness direction can be neglected. The measured temperature profile can be approximated by a fourth order polynomia,

$$T(r) = a_0 + a_2r^2 + a_4r^4$$

A finite element computation have been used in order to calculate the thermal fields in the sample. The data and assumptions taken into account are given as follows :

-the radial irradiation intensity profile (heat power) on the surface of the sample has been measured with a power meter, giving a Gaussian profile.

-the thermal conductivity of B_4C sample is taken as a function of the temperature. Its Young's modulus is a constant.

-considering the emissivity and the conductivity of the material, the heat power must be atenuated (10 factor).

A good correlation between measured and calculated temperatures is obtained (figure4) ; the thermocouple seems not to be disrupted by irradiation. The temperature gradient in the thickness direction can be neglected.

2.2.3. Thermal stresses calculation

The induced higher thermal expansion in the disc center is constrained by the cooler edge, leading to tensile hoop stresses at the periphery and tangential and radial compressive stresses in the center.

The stresses are calculated for plane stress conditions in axial direction because the ratio of the thickness to diameter of the discs is very small (t/D = 0.05). The linear elastic solution for tangential thermal stresses in an homogeneous material gives [6] :

$$\sigma_{\theta\theta} = \alpha E \left[\frac{1}{R^2}\int_0^R T\, r\, dr + \frac{1}{r^2}\int_0^r T\, r\, dr - T\right] \qquad (1)$$

The measured temperature profile approximated by a fourth order polynomia, $T(r) = a_0 + a_2 r^2 + a_4 r^4$, gives by integration for $r = R$:

$$\sigma_{\theta\theta max} = -a_2 \frac{R^2}{2} - 2a_4 \frac{R^4}{3} \qquad (2)$$

where T is the temperature, R the radius sample, E the Young's modulus and α the coefficient of thermal expansion.

Stress fields in the sample have been calculated by finite element computation (elastic calculation). The stresses are calculated for plane stress conditions ; only thermal stresses are taken into consideration.

Analytical formulations giving stresses from temperature profiles (1,2) are in good agreement with calculation (figure 4). Maxima tensile hoop stresses are located at the periphery, leadind to crack propagation from the periphery to the center.

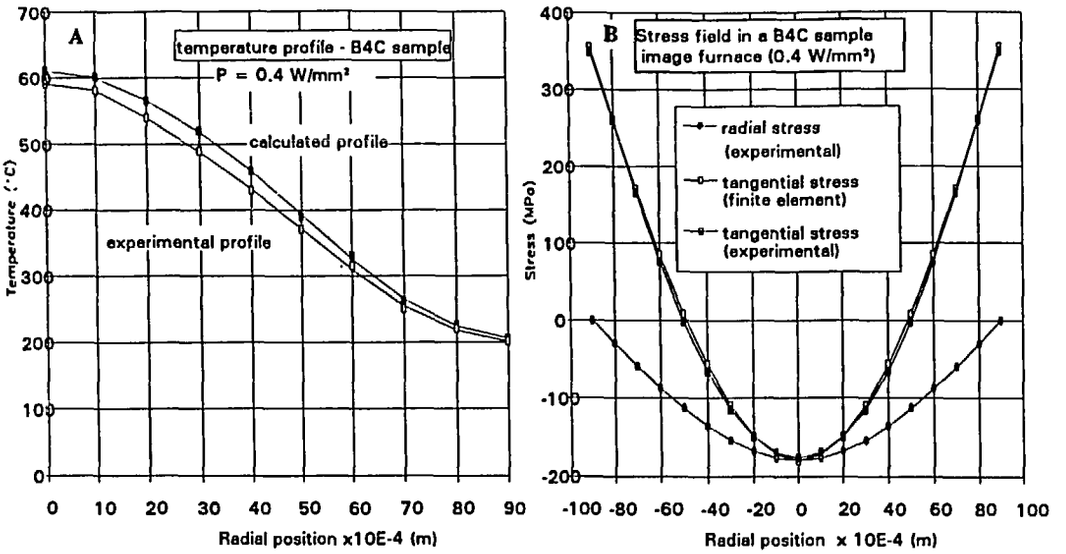

FIGURE 4
comparison of measured and calculated profiles, (A) temperature, (B) stresses

3. RESULTS AND DISCUSSION

3.1. Microstructures

Figure 5A shows the microstructure of the micro-dispersed B_4C-BN composite ; this figure is quite typical of the other micro-dispersed composites. Figure 5B/C/D illustrate respectively the structures of the macro-dispersed B_4C-Mo, B_4C-HfB_2 and B_4C-BN composites. The relative density of the composites is approximatively 96%.

The microstructures of micro-dispersed composites are homogeneous : the second phase is well dispersed in the B_4C matrix, and second phase and the grain size of each phase is quite similar (micronic grains).

In macro-dispersed composites, a more complex structure is observed ; the aggregates (100-500 μm) are roughly spherical. In the B_4C-HfB_2 composite, many cracks develop, resulting from the difference in dilatation coefficients of the phases : strong hoop compression stresses are developped in the B_4C matrix, whereas hoop and radial tensile stresses occur in the HfB_2 aggregates, depending on the size of the aggregates[7].

In the B_4C-Mo composite, EPMA has revealed a free carbon layer (30 μm) resulting from boron diffusion at the B_4C/Mo interface. In the B_4C-BN composite, we observe B_4C aggregates in a BN matrix. The BN phase is continuous even for contents as low as 10 vol %.

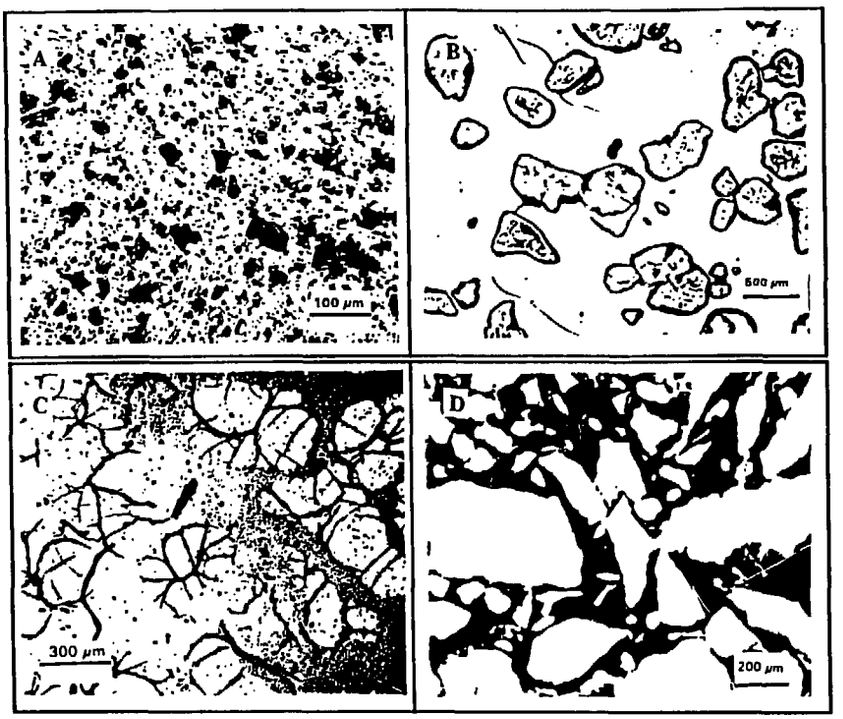

FIGURE 5
Microstructures of micro- and macro-dispersed composites
(A) micro-dispersed B_4C-BN 20 vol.%, (B) macro-dispersed B_4C-Mo, 20 vol.%, 300 μm aggregates, (C) macro-disperded B_4C-HfB_2 30 vol.%, 400 μm aggregates, (D) macro-dispersed B_4C-BN, 20 vol.%, B_4C aggregates.

3.2. Thermal shock

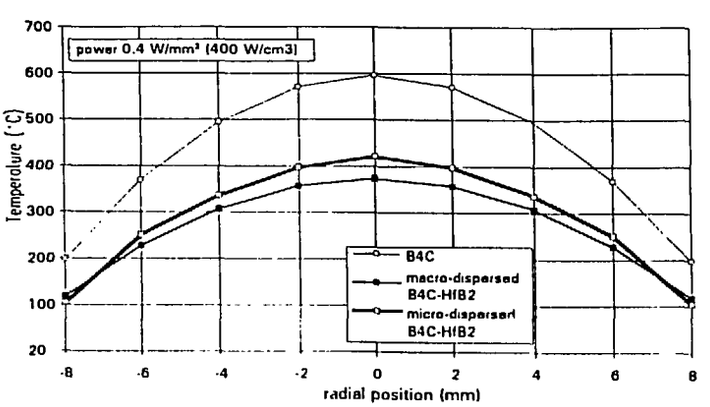

FIGURE 6
Temperature profiles of B_4C, micro- and macro-dispersed B_4C-HfB_2 composites

The obtained results are reported in table 2. The temperature profiles of micro- and macro-dispersed B_4C-HfB_2 are reported on figure 6.

	Crack initiation						ΔTc (°C)
	Heat power (W/mm^2)	center temp. (°C)	ΔTd (°C)	Thermal stress* (MPa)	Biaxial stress (MPa)	Aspect	
B_4C	5	550	350	360	370	broken	350
micro-dispersed composites :							
B_4C-Mo	12	640	430	520	530	broken	430
B_4C-HfB_2	10	710	500	405	410	broken	500
B_4C-BN	10	650	320	310	305	broken	320
macro-dispersed composites :							
B_4C-Mo	10	680	430	-	160	cracked	>550
B_4C-HfB_2	9	740	420	-	140	cracked	>560
B_4C-BN	13	800	480	-	160	cracked	>590

* : thin plate theory (equation (2))

TABLE 2
Thermal shock testing results of micro- and macro-dispersed composites
(ϕ 17 mm, t = 1 mm pellets)

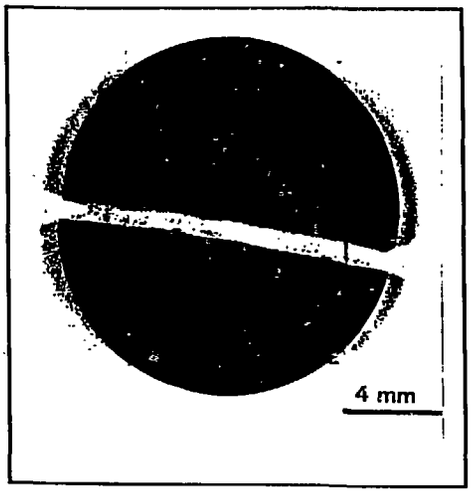

FIGURE 7A
Brittle fracture of a micro-dispersed composite submitted to the image furnace

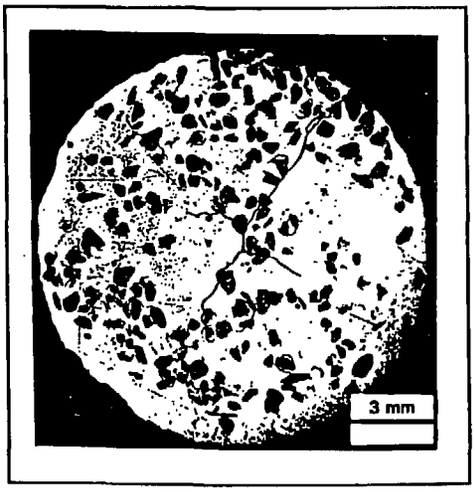

FIGURE 7B
Crack trapping in the macro-dispersed B_4C-HfB_2 composite

Micro-dispersed composites have a higher ΔTd than pure boron carbide, but present a catastrophic brittle behavior (figure 7a) ; in that case, ΔTd is equal to ΔTc.

Moreover, calculated thermal stresses corresponding to crack initiation are in a good agreement with biaxial flexure results performed on the same type of specimen[8].

The highest temperature drops for discs breaking are achieved by the macro-dispersed composites : those materials do not break, they only crack and cracks remain stable even for higher heating (ΔTc > ΔTd) (figure 7b).The pellets are indeed warped, but keep their integrity.

In the case of macro-dispersed composites, the stress fields existing locally around the aggregates cannot be approximated by the thin plate theory because of residual stresses and inhomogeneity ; hence, the application of equation (2) is not valid.

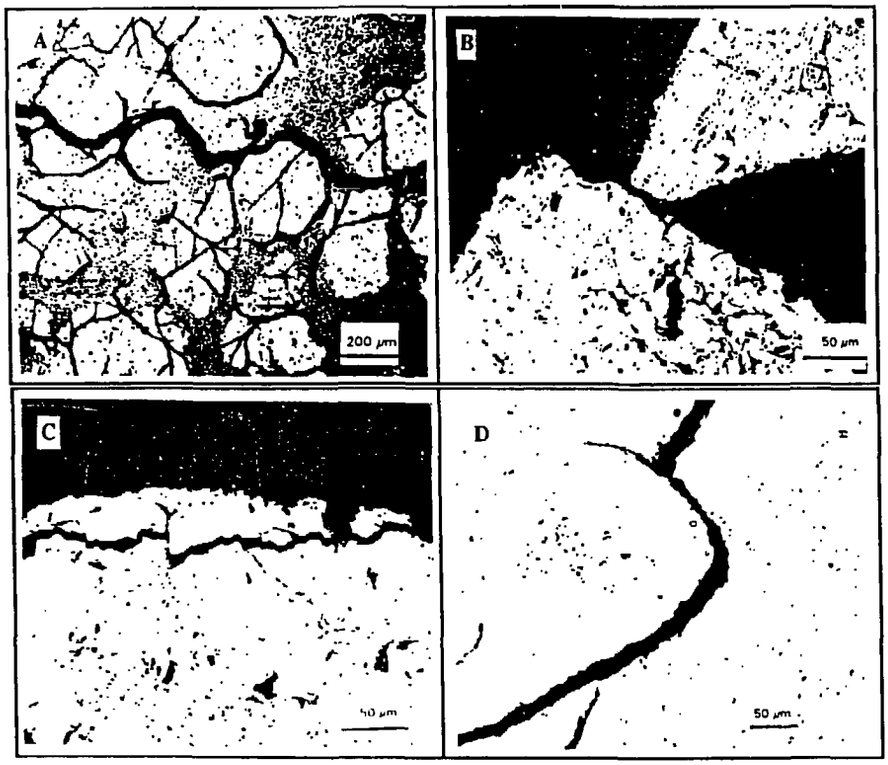

FIGURE 8

(A) deflection in macro-dispersed B_4C-HfB_2 (microcracking), (B) deflection in macro-dispersed B_4C-Mo (weak carbon interface). (C) crack bridging (Mo aggregate). (D) deflection by residual stress field (small uncracked HfB_2 aggregate).

Microstructural analyses of macro-dispersed composites after image furnace testing involve different toughening mechanisms. The toughening mechanisms can be subdivised into crack deflection (figure 8A/B) : the macro-crack moves across low energy path as microcracks or

weak carbon interface ; contact shielding processes as crack bridging (figure 8C) : the ductility of Mo aggregates induces closure forces on the wake of the crack ; and stress-induced shielding processes from residual stress fields (figure 8D) : local residual stresses in the vicinity of aggregates involve crack deflection. All these energy dissipating mechanisms reduce the crack driving force leading to a less brittle behaviour of the composite.

4. CONCLUSION

Ceramic-ceramic and ceramic-metal boron carbide based composites have been elaborated according to two processes leading to micro- and macro-dispersed microstructures. thermomechanical tests, performed by mean of an image furnace show that micro-dispersed composites remain purely brittle : strength and Young's modulus are improved but catastrophic failure is inescapable. These materials seem not be able to prevent the splitting of the neutron absorber pellets.

On the other hand, a significant improvement of thermo-mechanical properties of composites has been observed with a macro-dispersed microstructure : aggregates lead to different toughening mechanisms. In these composites, cracks remain subcritical and propagate at short range ; the pellets keep their integrity because of the presence of residual stresses and weak interface which trap thermal cracks. At least, selected materials will be neutron irradiated to confirm whether their structure allows a significantly improved behavior under irradiation.

REFERENCES

1) T. STOTO, N. HOUSSEAU, L. SUPPIROLI, B. KRYGER, J. Appl. Phys. **68-2** (1990)3198-3206
2) L. ZUPPIROLI, D. LESUEUR, Phil. Mag. A **60-5**(1989)539-551
3) G.W. HOLLENBERG, Ceramic Bulletin vol.**59,5**(1980)538-546
4) G.M. DECROIX, D. GOSSET, B. KRYGER, Matériau absorbant les neutrons et son procédé de fabrication : B_4C-HfB_2, French Patent 93 06304
5) G.M. DECROIX, J. CHATILLON, D. NOAILLAC, Y. FRASLIN, Matériaux absorbants les neutrons et leur procédé de fabrication : B_4C-Mo et B_4C-BN, French Patent 9314873
6) S. P. TIMOSHENKO, J. N. Goodier, theory of elasticity (Mc Graw Hill-Gogakusha)
7) K. T. FABER, T. IWAGOSHI, A. GHOSH, J. Am. Ceram. Soc., **71-9**(1988)C399-C401
8) G.M. DECROIX et al., to be published.